Nem 10-00142

Molecular and morphological characterisations of two new species of *Rotylenchus* (Nematoda: Hoplolaimidae) from Iran

Mohammad Reza ATIGHI[1], Ebrahim POURJAM[2,*], Majid PEDRAM[2], Carolina CANTALAPIEDRA-NAVARRETE[3], Juan E. PALOMARES-RIUS[3] and Pablo CASTILLO[3]

[1] *Department of Plant Protection, Faculty of Agricultural Sciences and Engineering, University College of Agriculture and Natural Resources, University of Tehran, Karaj, Iran*

[2] *Plant Pathology Department, College of Agriculture, Tarbiat Modares University, Tehran, Iran*

[3] *Institute for Sustainable Agriculture (IAS), Spanish National Research Council (CSIC), Alameda del Obispo s/n, Apdo. 4084, 14080 Córdoba, Spain*

Received: 2010; revised: March 2011

Accepted for publication: March 2011

* Corresponding author, e-mail: Pourjame@modares.ac.ir

Summary – Two new amphimictic species, *Rotylenchus iranicus* n. sp. and *R. conicaudatus* n. sp. are described. *Rotylenchus iranicus* n. sp. is characterised mainly by an offset hemispherical lip region with 5-6, rarely 7 annuli, stylet 39-44 µm long, vulva located at 53-65% and rounded tail with 4-9 annuli and typical smooth tip. Morphologically this species is related to *R. montanus*, *R. provincialis* and *R. aqualamus*. *Rotylenchus conicaudatus* n. sp. is characterised mainly by a slightly offset conoid-rounded lip region with 4-5, rarely 6, annuli, stylet 27-32 µm long, vulva located at 52-63% and conoid-rounded tail with 10-16 annuli and a typical annulated tip. Morphologically this species is related to *R. pumilus*, *R. abnormecaudatus*, *R. acuspicaudatus* and *R. provincialis*. The results of the phylogenetic analysis based on sequences of the D2-D3 expansion regions of 28S and ITS1-rRNA genes confirmed the species differentiation. Phylogenetic relationships with other species were difficult to assign using D2-D3 expansion regions of 28S. However, using ITS1-rRNA, *R. conicaudatus* n. sp. presented a close relationship with *R. unisexus*, whilst *R. iranicus* n. sp. was closely related to *R. conicaudatus* n. sp., *R. unisexus*, *R. incultus* and *R. laurentinus*.

Keywords - D2-D3, oriental beech tree, molecular, morphology, morphometrics, phylogeny, *Rotylenchus conicaudatus* n. sp., *Rotylenchus iranicus* n. sp., spiral nematodes, taxonomy.

In the past 5 years, several authors have contributed to our knowledge of the taxonomy and distribution of *Rotylenchus* Filipjev, 1936 (Castillo & Vovlas, 2005; Vovlas *et al*., 2008), although it is still poorly known in Iran (Geraert & Barooti, 1996; Gharakhani *et al*., 2009). During nematode surveys conducted in cultivated and natural environments in northern Iran, two amphimictic spiral nematodes were detected in the rhizosphere of oriental beech trees (*Fagus orientalis* Lipsky) in the Research Forest of Tarbiat Modarres University, Sisangan, and in the rhizosphere of undetermined grasses in Azad Kooh Mountain (4234 m a.s.l.), both in Mazandaran province, northern Iran. Preliminary morphological examinations indicated that these two species did not fit any description of known *Rotylenchus* species and appeared to be morphologically related to *R. montanus* Vovlas, Subbotin, Troccoli, Liébanas & Castillo, 2008 and *R. pumilus* (Perry *in* Perry, Darling & Thorne, 1959) Sher, 1961. The objectives of this paper were: *i*) to verify the taxonomic status of these species, conducting morphometric and molecular studies of these unknown *Rotylenchus* species, which are described here in as *Rotylenchus iranicus* n. sp. and *R. conicaudatus* n. sp.; and *ii*) to determine the molecular phylogenetic affinities of *R. iranicus* n. sp. and *R. conicaudatus* n. sp. with closely related species using the rRNA gene sequences (ITS1-rRNA and D2-D3 of 28S).

Material and methods

NEMATODE POPULATIONS

Specimens of *R. iranicus* n. sp. were obtained from the rhizosphere of forest trees in the Research Forest of University of Tarbiat Modarres, Sisangan, Mazandaran Province, northern Iran. Material of *R. conicaudatus* n. sp. was collected in the rhizosphere of undetermined grasses in Azad Kooh Mountain (4234 m a.s.l.), Mazandaran province, northern Iran. The nematodes were extracted from soil samples by the centrifugal-flotation method (Jenkins, 1964).

Specimens for light microscopy (LM) were killed by gentle heat, fixed in a solution of 4% formaldehyde + 1% propionic acid and processed to pure glycerin using De Grisse's (1969) method. Specimens were examined using a Zeiss III compound microscope with Nomarski differential interference contrast at up to ×1000 magnification. Measurements were done using a *camera lucida* attached to a Nikon

Eclipse E600 light microscope. For line drawing, handmade drawings were scanned and imported to CorelDraw software version 12 and redrawn. Morphometric data were processed using Statistix 9.0 (NH Analytical Software, Roseville, MN, USA).

DNA EXTRACTION, PCR, CLONING AND SEQUENCING

Nematode DNA from *R. iranicus* n. sp. and *R. conicaudatus* n. sp. was extracted from single individuals using proteinase K as described by Castillo *et al*. (2003). Detailed protocols for PCR and sequencing were as described by Castillo *et al*. (2003). The following primers were used for amplification D2A (5'-ACAAGTACCGTGAGGGAAAGTTG-3') and D3B (5'-TCGGAAGGAACCAGCTACTA-3') for amplification of D2-D3 regions of 28S (Subbotin *et al.*, 2006); and TW81 (5´-GTTTCCGTAGGTGAACCTGC-3´) and 5.8SM5 (5´-GGCGCAATGTGCATTCGA-3´) for amplification of the ITS1-rRNA (Vovlas *et al*., 2008). Both sequences were amplified and used for sequence and phylogenetic analysis.

PCR products were purified after amplification with Geneclean turbo (Q-BIOgene SA, Illkirch Cedex, France) or QIAquick (Qiagen, USA) gel extraction kits, quantified using a Nanodrop spectrophotometer (Nanodrop Technologies, Wilmington, DE, USA) and used for direct sequencing in both directions with the primers referred above. The resulting products were purified and run on a DNA multicapillary sequencer (Model 3100 genetic analyser; Applied Biosystems, Foster City, CA, USA) at the STABVIDA sequencing facilities (Monte da Caparica, Portugal). The newly obtained sequences were submitted to the GenBank database under accession numbers HQ700697-HQ700700 as indicated on the phylogenetic trees.

PHYLOGENETIC ANALYSES

D2-D3 expansion segments of 28S and ITS1-rRNA newly obtained sequences and sequences obtained from GenBank were used for phylogenetic reconstruction. Outgroup taxa for each dataset were chosen according to previous published data (Vovlas *et al*., 2008) for D2-D3 expansion regions of 28S rRNA. The newly obtained and published sequences for each gene were aligned using ClustalW (Thompson *et al*., 1997) with default parameters. Sequence alignments were manually edited using

BioEdit (Hall, 1999). Phylogenetic analysis of the sequence data sets were performed with maximum likelihood (ML) using PAUP * 4b10 (Swofford, 2003) and Bayesian inference (BI) using MrBayes 3.1.2 (Huelsenbeck & Ronquist, 2001). The best fit model of DNA evolution was obtained using the program JModelTest ver. 0.1.1 (Posada, 2008) with the Akaike Information Criterion (AIC). The Akaike-supported model, the base frequency, the proportion of invariable sites and the gamma distribution shape parameters and substitution rates in the Akaike information criterion (AIC) were used in phylogenetic analyses. BI analysis under TVM + I + G model for the D2-D3 expansion segment of 28S rDNA and TVM + G for the ITS1 region was initiated with a random starting tree and was run with four chains for 2.0×10^6 generations. The Markov chains were sampled at intervals of 100 generations. Two runs were performed for each analysis. After discarding burn-in samples and evaluating convergence, the remaining samples were retained for further analysis. The topologies were used to generate a 50% majority rule consensus tree. Posterior probabilities (PP) are given on appropriate clades. Trees were visualised using TreeView program (Page, 1996). In ML analysis, the estimation of the support for each node was made using a bootstrap analysis with 100 fast-step replicates.

Descriptions

***Rotylenchus iranicus** n. sp.**

(Figs 1, 2)

MEASUREMENTS

See Table 1.

DESCRIPTION

Female

Body habitus upon relaxation C-shaped to open spiral, cuticular annuli 1.7 ± 0.5 (1.5-2.5) µm wide. Body without any longitudinal striations. Lip region hemispherical,

*The species epithet refers to the country were the species was found.

offset, with 5-6, rarely 7, annuli, 11.8 ± 0.8 (11.0-13.0) µm broad, 7.8 ± 0.7 (7.0-9.0) µm high. Lateral fields with four, smooth equidistant lines, beginning anteriorly at annulus 4-7 as three lines forming two bands, after 18-27 annuli, central line dividing to form a third band. The three bands are 8.7 ± 2.1 (7-11) µm wide at mid-body, *ca* one fifth as wide as body diam. Regular areolation of lateral fields (external bands) observed in pharyngeal region. Labial framework strongly developed. Outer margin of labial framework extending *ca* 1.5-2.0 body annuli to posterior basal plate. Stylet robust with rounded basal knobs 6.5-8.0 µm wide. Orifice of dorsal pharyngeal gland opening at 5.5-10.0 µm posterior to stylet base. Procorpus cylindrical, narrowing slightly at junction with median pharyngeal bulb, 75-96 µm long. Median pharyngeal bulb broadly oval (13 ×19 µm), with well developed valvular apparatus 3.5-4.0 µm long, located at 59.6-72.7% of pharyngeal length. Nerve ring enveloping isthmus at mid-point, 98-113 µm from anterior end. Excretory pore position varying from anterior to posterior to pharyngo-intestinal valve (in one specimen, pore posterior to end of overlap). Pharyngeal glands sacciform, with three nuclei, overlap short, *ca* 3-16 µm long. Hemizonid distinct, located anterior to excretory pore, extending for *ca* 1.5-2.0 body annuli. Reproductive system with two equally developed genital branches, anterior branch 210 ± 45.6 (135-273) µm long, posterior branch 220 ± 42.9 (173-321) µm long, respectively 19.2 ± 3.9 (12.5-25.3) and 20.2 ± 4.1 (14.6-29.7)% of body length. Ovaries with a single row of oocytes. Vulva slightly posterior to mid-body, with a short epiptygma 1-1.5 µm long. Spermatheca almost spherical, 15-27 diam., functional, with rounded sperm. Phasmid pore like, located at 5-13 annuli anterior to anus and 26-38 µm from tail tip. Tail short, rounded, slightly conoid in some specimens, *ca* 0.5 anal body diam. long with smooth tip.

Male

Common, almost as abundant as female. Morphology similar to that of female, except for sexual dimorphism. Lip region as in female, but slightly more elevated in outline, 5.5-8.5 µm broad, 10-12 µm high. Stylet knobs less developed compared to that of female (5.5-7.5 µm wide). Testis single, anteriorly outstretched 379 ± 60 (286-469) µm long. Spicules slightly cephalated, ventrally arcuate. Gubernaculum non-protrusible, with prominent titillae distally. Bursa crenate, well developed, enveloping tail terminus,

67 ± 3.0 (62-71) µm long. Tail tapering, terminus rounded-pointed. Phasmid on bursa at level of cloacal aperture.

TYPE HOST AND LOCALITY

Rotylenchus iranicus n. sp. was found in a clay soil around oriental beech trees (*Fagus orientalis* Lipsky), Sisangan forest, Mazandaran province, northern Iran.

TYPE MATERIAL

Holotype female, five female and five male paratypes deposited in the Nematode Collection of the Faculty of Agriculture, Tarbiat Modares University, Tehran-Iran. Two female and two male paratypes deposited at each of the following collections: CABI Europe-UK, Egham, Surrey, UK; Istituto per la Protezione delle Piante (IPP) of Consiglio Nazionale delle Ricerche (C.N.R.), Sezione di Bari, Bari, Italy; USDA Nematode Collection, Beltsville, MD, USA. Specific D2-D3 and ITS1-rRNA sequences deposited in GenBank with accession numbers HQ700697 and HQ700699, respectively.

DIAGNOSIS AND RELATIONSHIPS

Rotylenchus iranicus n. sp. is a bisexual species and is assigned to the species group having a hemispherical lip region, rounded female tail and stylet more than 40 µm long (Castillo & Vovlas 2005). It is characterised mainly by an offset hemispherical lip region with 5-6, rarely 7 annuli, stylet length of 39-44 µm, vulva position at 53-65%, rounded tail with 4-9 annuli and a specific D2-D3 and ITS1-rRNA sequence (GenBank accession numbers HQ700697 and HQ700699, respectively).

Morphologically *R. iranicus* n. sp. can be distinguished from the most similar species by a number of particular characteristics resulting from its specific matrix code (A4, B1, C1, D4, E4, F3, G2, H2, I2, J1, K2 *sensu* Castillo & Vovlas, 2005). From *R. montanus* it differs by distance of dorsal pharyngeal gland orifice to stylet base (5.5-10.0 *vs* 4.0-5.5 µm), stylet length (39-44 µm *vs* 32.5-36.5 µm), pharyngeal gland overlap (3-16 *vs* 18-31 µm), female tail shape (short, rounded, slightly conoid in some specimens with typically smooth terminus *vs* rounded, often with a slight depression on dorsal margin, tail terminus regularly annulated), and males common *vs* absent in *R.*

montanus. From *R. provincialis* Scotto La Massèse & Germani, 2000 it differs by lip region shape (hemispherical *vs* broadly rounded), distance of dorsal pharyngeal gland orifice to stylet base (5.5-10.0 *vs* 4.0-7.5 µm), stylet length (39-44 *vs* 30.5-33.0 µm), pharyngeal gland overlap (3-16 *vs* 21-25 µm), female tail shape (short, rounded, slightly conoid in some specimens and typically smooth terminus *vs* convex-conoid, tail terminus smooth), and males common *vs* absent in *R. provincialis*. From *R. aqualamus* Van den Berg, Marais & Tiedt, 2007 it differs by lip region shape (hemispherical *vs* rounded), lip region annuli (5-7 *vs* 4), stylet length (39-44 *vs* 26-28 µm), stylet knob shape (rounded *vs* grape-stone-like), lateral fields (non-areolated *vs* irregularly areolated over whole length of body), and males common *vs* absent in *R. aqualamus*. From *R. acuspicaudatus* Van den Berg & Heyns, 1974 it differs by lip region shape (hemispherical *vs* broadly rounded), stylet length (39-44 *vs* 26.0-28.5 µm), and female tail shape (short, rounded, slightly conoid in some specimens and typically smooth terminus *vs* pointed on ventral side).

***Rotylenchus conicaudatus*[*] n. sp.**

(Figs 3, 4)

MEASUREMENTS

See Table 2.

DESCRIPTION

Female

Body habitus upon relaxation C-shaped to open spiral, with cuticular annuli 1.8 ± 0.2 (1.5-2.0) µm wide. Body without longitudinal striations in any region. Lip region conoid-rounded, slightly offset, with 4-5, rarely 6, annuli, 8.7 ± 0.5 (8.0-9.0) µm wide, 4.7 ± 0.4 (4.0-5.0) µm high. Lateral fields with four, smooth equidistant lines. The three bands are 8.7 ± 1.6 (7-14) µm wide at mid-body, *ca* one-third as wide as body diam. Regular areolation of lateral fields (external bands) observed in pharyngeal region.

[*]The species epithet is formed from the Latin *conus* = cone, and *caudatus* = tailed, and refers to shape of the conoid tail.

Labial framework strongly developed. Outer margin of labial framework extending *ca* 1-1.5 body annuli posterior to basal plate. Stylet robust with rounded basal knobs 5.0-6.5 µm wide. Orifice of dorsal pharyngeal gland opening at 6.5-11.0 µm posterior to stylet base. Procorpus cylindrical, narrowing slightly at junction with median pharyngeal bulb, 41-61 µm long. Median pharyngeal bulb broadly oval (13.5 × 16.0 µm), with well developed valvular apparatus 3.0-3.5 µm long, located 53-55% of pharyngeal length. Nerve ring enveloping isthmus at mid-point, 101-105 µm from anterior end. Excretory pore located anterior to pharyngo-intestinal valve. Pharyngeal glands sacciform, with three nuclei, overlapping intestine dorsally and ventro-laterally, overlap *ca* 19-33 µm long. In four specimens, a ventro-lateral overlap was more developed. Hemizonid distinct, located anterior to excretory pore, extending for *ca* 1.0-1.5 body annuli. Reproductive system with two equally developed genital branches, anterior branch 216 ± 44.8 (144-277) µm long, posterior branch 238 ± 44.8 (163-298) µm long, respectively 23.5 ± 4.9 (14.6-29.8) and 25.7 ± 3.2 (18.5-29.2)% of body length. Ovaries with single row of oocytes. Vulva slightly posterior to mid-body, epiptygma absent. Spermatheca almost spherical, 14-22 diam., functional with rounded sperm (2-2.5 µm diam.). Phasmid pore like, located at 5-12 annuli anterior to anus and 32-43 µm from tail tip. Tail short, conoid-rounded, *ca* one anal body diam. long, with annulated tip.

Male

Rare, only one specimen was detected. Morphology similar to that of female, except for sexual dimorphism. Lip region as in female, but slightly more elevated in outline, 5.0 µm wide × 8.0 µm high. Stylet knobs less developed compared to that of female (4.0 µm wide). Testis single, anteriorly outstretched. Spicules slightly cephalated, ventrally arcuate. Gubernaculum non-protrusible. Bursa crenate, well developed, 71 µm long, enveloping tail terminus. Tail tapering with a rounded-pointed tip. Phasmid on bursa, located at cloacal aperture level.

TYPE HOST AND LOCALITY

Rotylenchus conicaudatus n. sp. was found in the rhizosphere of undetermined grasses in Azad Kooh Mountain (4234 m a.s.l.), Mazandaran province, northern Iran.

TYPE MATERIAL

Holotype female, paratype male and five paratype females deposited at Nematode Collection of the Faculty of Agriculture, Tarbiat Modares University, Tehran-Iran. Two female paratypes deposited at each of the collections indicated for *R. iranicus* n. sp. Specific D2-D3 and ITS1-rRNAsequences deposited in GenBank with accessions numbers HQ700698 and HQ700700, respectively.

DIAGNOSIS AND RELATIONSHIPS

Rotylenchus conicaudatus n. sp. is a bisexual species assigned to the species group having a conoid-rounded lip region with 4-5 annuli, lateral field areolated only in pharyngeal region, stylet 30-35.9 µm long, and a conoid-rounded female tail (Castillo & Vovlas 2005). It is characterised mainly by a slightly offset conoid-rounded lip region with 4-5, rarely 6, annuli, stylet 27-32 µm long, vulva located at 52-63%, conoid-rounded tail with 10-16 annuli, and specific D2-D3 and ITS1-rRNA sequences (GenBank accession numbers HQ700698 and HQ700700, respectively).

Morphologically, *R. conicaudatus* n. sp. can be distinguished from the most similar species by a number of particular characteristics resulting from its specific matrix code (A3, B2,3, C1, D4, E2, F3, G3, H2,3, I2, J1, K1 *sensu* Castillo & Vovlas, 2005). From *R. pumilus* it differs by a longer body (0.76-1.05 *vs* 0.5-0.7 mm), female tail shape (conoid-rounded *vs* almost hemispherical), and position of phasmids (5-12 annuli anterior to anus *vs* usually located immediately posterior to anus). From *R. abnormecaudatus* Van den Berg & Heyns, 1974 it differs by a longer body (0.76-1.05 *vs* 0.6-0.7 mm), lip region shape (conoid-rounded *vs* broadly rounded), longer stylet (27-32 *vs* 24-25 µm), female tail shape (conoid-rounded with 10-16 annuli *vs* irregularly rounded with 8-11 annuli irregularly arranged at terminus), and males present and spermatheca functional *vs* absent, spermatheca absent. From *R. acuspicaudatus* it differs by lip region shape (conoid-rounded *vs* broadly rounded), female tail shape (conoid-rounded with 10-16 annuli *vs* pointed on ventral side with 13-16 annuli) and longer male tail (23-28 *vs* 12.9-16.2 µm) with well crenated bursa *vs* fringe-like appearance of the annulus on the posterior part of the bursa. From *R. provincialis* it differs by lip region shape (conoid-rounded *vs* broadly rounded), female tail shape (conoid-rounded

with 10-16 annuli *vs* convex-conoid with 8-10 annuli, rounded and not annulated at the tip,).

PHYLOGENETIC POSITION OF *R. IRANICUS* N. SP. AND *R. CONICAUDATUS* N. SP. WITHIN THE GENUS

The primer pairs of D2A and D3B, TW81 and 5.8SM5 amplified a PCR product 750 bp and 800 bp in length based on gel images, respectively. *R. iranicus* n. sp. differed in the D2-D3 sequence from the most closely related species, *R. conicaudatus* n. sp. by 70 nucleotides (92% similarity, 709/779 identities) and 22 gaps (2%, 29/779), from *R. agnetis* Szczygiel, 1968 (EU280795), by 54 nucleotides (91% similarity, 519/573 identities) and 18 gaps (3%, 18/573), from *R. magnus* Zancada, 1985 (EU280790), by 57 nucleotides (91% similarity, 517/574 identities) and 16 gaps (2%, 16/574), from *R. robustus* (de Man, 1876) Filipjev, 1936 (EU280788), by 57 nucleotides (91% similarity, 517/573 identities) and 19 gaps (3%, 19/573), and finally, from *R. uniformis* (Thorne, 1949) Loof & Oostenbrink, 1958 (DQ328739) by 57 nucleotides (91% similarity, 516/573 identities) and 19 gaps (3%, 19/573). *Rotylenchus conicaudatus* n. sp. differed in the D2-D3 sequence from the most closely related species, *R. iranicus* n. sp., by 70 nucleotides (92% similarity, 709/779 identities) and 22 gaps (2%, 29/779), from *R. robustus* (EU280788), by 50 nucleotides (92% similarity, 518/568 identities) and nine gaps (1%, 9/568), from *R. eximius* Siddiqi, 1964 (DQ328741) by 51 nucleotides (92% similarity, 518/569 identities) and 11 gaps (1%, 11/569), and finally, from *R. uniformis* (DQ328739), by 51 nucleotides (92% similarity, 517/568 identities) and nine gaps (1%, 9/568). Differences in the amplified fragment of ITS1-rRNA sequences yield wider differences than the amplified D2-D3 fragments. *Rotylenchus iranicus* n. sp. closest species in ITS1 sequence was *R. conicaudatus* n. sp., by 261 nucleotides (70% similarity, 499 identities) and 47 gaps (7%, 47/713). The remainder of *Rotylenchus* species differ between 338-370 and 379-384 nucleotides for *R. iranicus* n. sp. and *R. conicaudatus* n. sp., respectively, from the aligned sequences with prior elimination of ambiguously aligned regions.

The D2-D3 alignment consisted of 51 sequences of 570 bp in length. The 50% majority rule consensus phylogenetic tree generated from the D2-D3 alignment by BI analysis under the TVM + I + G model is presented in Figure 5. The tree topologies between ML and BI were congruent. This tree topology was similar to that obtained by

Vovlas *et al*. (2008) with the complex model using secondary structures. Small differences may be due to the different phylogenetic methods and additional sequences added in our study. Some major clades were not well defined in our tree, but it showed the paraphyly of Hoplolaimidae (Subbotin *et al*., 2007, Vovlas *et al*., 2008). *Rotylenchus iranicus* n. sp. and *R. conicaudatus* n. sp. did not form supported clades with any of the other *Rotylenchus* species, occupying paraphyletic positions between the other genus included in the analysis. The ITS1-rRNA alignment consisted of 25 sequences with 433 bp, after discarding ambiguously aligned regions from the alignment. The 50% majority rule consensus phylogenetic tree generated from the ITS1-rRNA alignment by BI analysis under the TVM + G model is presented in Figure 6. The tree topologies between ML and BI were congruent. This tree was similar to that obtained by Vovlas *et al*. (2008), although the position of *R. eximius* in our tree differed when using *Hoplolaimus columbus* (DQ309584) as outgroup. The position of *R. iranicus* n. sp. and *R. conicaudatus* n. sp. were well defined. *Rotylenchus conicaudatus* n. sp. formed a highly supported clade by BI analysis with *R. unisexus* Sher, 1965 (EU373675 and EU373674), whilst *R. iranicus* n. sp. formed a supported clade including *R. conicaudatus* n. sp., *R. unisexus* (EU373675 and EU373674), *R. laurentinus* Scognamiglio & Talamé, 1973 (EU373666 and EU373667) and *R. incultus* Sher, 1965 (EU373672 and EU373673). Since *R. iranicus* n. sp. was similar morphologically to *R. montanus*, this relationship agrees with the position of both species in the ITS1-rRNA tree, in which *R. montanus* is present in one of the major clades that includes *R. iranicus* n. sp. Vovlas *et al* (2008) found that morphological similarities associated with the phylogeny of *Rotylenchus* using ribosomal regions were difficult to assign in some species lineages (*R. goodeyi* Loof & Oostenbrink, 1958, *R. incultus* and *R. laurentinus*) and with *R. unisexus*, whilst in other related lineages (*R. montanus* and *Rotylenchus* sp.) there were some common characters. We obtained similar conclusions when including *R. iranicus* n. sp. and *R. conicaudatus* n. sp.

Acknowledgements

The authors thank the excellent technical assistance of J. Martín Barbarroja (IAS-CSIC).

References

CASTILLO, P. & VOVLAS, N. (2005). *Bionomics and identification of the genus* Rotylenchus *(Nematoda: Hoplolaimidae)*. Nematology Monographs and Perspectives, vol. 3 (series editors: Hunt, D.J. & Perry, R.N.). Leiden, The Netherlands, Brill Academic Publishers, 377 pp.

CASTILLO, P., VOVLAS, N., SUBBOTIN, S. & TROCCOLI, A. (2003). A new root-knot nematode, *Meloidogyne baetica* n. sp. (Nematoda: Heteroderidae), parasitizing wild olive in Southern Spain. *Phytopathology* 93, 1093-1102.

GERAERT, E. & BAROOTI, SH. (1996). Four *Rotylenchus* from Iran, with a key to the species. *Nematologica* 42, 503-520.

GHARAKHANI, A., POURJAM, E. & KAREGAR, A. (2009). Some tylenchid nematodes from Kerman province, Iran. Journal of *Plant Pests and Diseases* 77, 95-117.

DE GRISSE, A.T. (1969). Redescription ou modifications de quelques techniques utilisées dans l'étude des nématodes phytoparasitaires. *Mededelingen Faculteit Landbouwwetenschappen Rijksuniversiteit Gent* 34, 351-369.

JENKINS, W.R. (1964). A rapid centrifugal flotation technique for separating nematodes from soil. *Plant Disease Reporter* 48, 692.

HALL, T.A. (1999). BioEdit: a user-friendly biological sequence alignment editor and analysis program for windows 95/98/NT. *Nucleic Acids Symposium Series* 41, 95-98.

HUELSENBECK, J.P. & RONQUIST, F. (2001). MrBAYES: Bayesian inference of phylogenetic trees. *Bioinformatics* 17, 754-755.

PAGE, R.D.M. (1996). TREEVIEW: an application to display phylogenetic trees on personal computers. *Computer Applications in the Biosciences* 12, 357-358.

POSADA, D. (2008). JModelTest: Phylogenetic model averaging. *Molecular Biology and Evolution* 25, 1253-1256.

SCOTTO LA MASSÈSE, C. & GERMANI, G. (2000). Description de quatre nouvelles espèces et de quatre populations de *Rotylenchus* (Nematoda: Hoplolaimidae). Proposition d'une clé tabulaire. *Nematology* 2, 699-718.

SHER, S.A. (1961). Revision of the Hoplolaiminae (Nematoda). I. Classification of nominal genera and nominal species. *Nematologica* 6, 155-169.

SIDDIQI, M.R. (2000). *Tylenchida parasites of plants and insects*. 2nd edition. Wallingford, UK, CABI Publishing, 833 pp.

SUBBOTIN, S.A., STURHAN, D., CHIZHOV, V.N., VOVLAS, N. & BALDWIN, J.G. (2006). Phylogenetic analysis of Tylenchida Thorne, 1949 as inferred from D2 and D3 expansion fragments of the 28S rRNA gene sequences. *Nematology* 8, 455-474.

SUBBOTIN, S. A., STURHAN, D., VOVLAS, N., CASTILLO, P., TANYI TAMBE, J., MOENS, M. & BALDWIN, J.G. (2007). Application of the secondary structure model of rRNA for phylogeny: D2-D3 expansion segments of the LSU gene of plant-parasitic nematodes from the family Hoplolaimidae Filipjev, 1934. *Molecular Phylogenetics and Evolution* 43, 881-890.

SWOFFORD, D.L. (2003). PAUP*: Phylogenetic analysis using parsimony (*and other methods), version 4.0b 10. Sunderland, MA, USA, Sinauer Associates.

THOMPSON, J.D., GIBSON, T.J., PLEWNIAK, F., JEANMOUGIN, F. & HIGGINS, D.G. (1997). The CLUSTAL_X windows interface: flexible strategies for multiple sequence alignment aided by quality analysis tools. *Nucleic Acids Research* 25, 4876-4882.

VAN DEN BERG, E. & HEYNS, J. (1974). South African Hoplolaiminae 3. The genus *Rotylenchus* Filipjev, 1936. *Phytophylactica* 6, 165-184.

VAN DEN BERG, E., MARAIS, M. & TIEDT, L.R. (2007). Plant nematodes in South Africa. 9. Check-list of plant nematodes from the Goegap and Witsand Nature Reserves, Northern Cape Province, with a description of a new *Rotylenchus* species (Hoplolaimidae: Nematoda). *African Plant Protection* 13, 28-35.

VOVLAS, N., SUBBOTIN, S.A., TROCCOLI, A., LIÉBANAS, G. & CASTILLO, P. (2008). Molecular phylogeny of the genus *Rotylenchus* (Nematoda, Tylenchida) and description of a new species. *Zoologica Scripta* 37, 521-537.

1 **Table 1.** *Morphometrics of* Rotylenchus iranicus *n. sp. All measurements are in µm and*
2 *in the form: mean ± s.d. (range).*
3

Character	Female		Male
	Holotype	Paratypes	Paratypes
n	–	20	15
L	1237	1098 ± 79.6 (954-1237)	947 ± 62.3 (837-1044)
a	25.8	24.9 ± 2.1 (21.6-28.4)	27.7 ± 3.1 (22.8-32.2)
b	8.2	7.7 ± 0.5 (6.7-8.5)	6.7 ± 0.4 (6.1-7.4)
b'	7.6	7.3 ± 0.5 (6.5-8.3)	6.3 ± 0.4 (5.7-6.8)
c	82.5	82.3 ± 20.6 (53-120.4)	36.9 ± 2.9 (30.8-41)
c'	0.4	0.5 ± 0.1 (0.4-0.8)	1.2 ± 0.1 (1.0-1.4)
V or T	55.8	57.6 ± 2.7 (53-65)	40 ± 4.8 (33-47)
Stylet	43.0	42.1 ± 1.5 (39-44)	40.1 ± 1.0 (38-41.5)
Stylet conus	23.0	22.4 ± 1.0 (20-24)	21.3 ± 1.0 (19-23)
DGO	7.0	7.8 ± 1.6 (5.5-10)	7.8 ± 1.6 (5.0-10)
O	16.3	18.4 ± 3.8 (13.1-24.7)	19.4 ± 3.9 (12.2-24.4)
Anterior end to centre of median bulb	96.0	94 ± 6.4 (82-105)	89 ± 3.3 (84-97)
Anterior end to excretory pore	155.0	143 ± 9.8 (122-165)	133 ± 4.8 (126-140)
Pharynx length	151.0	143 ± 8.7 (128-156)	141 ± 5.4 (133-154)
Pharyngeal overlap	11.0	8.5 ± 3.7 (3.0-16)	9.9 ± 4.9 (3-22)
Max. body diam.	48.0	44.3 ± 4.7 (38-55)	34.5 ± 3.6 (27-39.5)
Anal/cloacal body diam.	36.0	25.8 ± 3.4 (22-36)	21.1 ± 1.3 (18-23)
Tail	15.0	14.2 ± 3.9 (9-23)	25.7 ± 2.0 (23-28)
Tail annuli	6.0	6.8 ± 1.4 (4-9)	–
Phasmid to terminus	29.0	32.2 ± 3.4 (26-38)	24.9 ± 2.0 (22-28)
Spicules	–	–	39.7 ± 1.9 (36-43)
Gubernaculum	–	–	16.6 ± 0.9 (15.5-18)

4
5

1 **Table 2.** *Morphometrics of* Rotylenchus conicaudatus *n. sp. All measurements are in*
2 *µm and in the form: mean ± s.d. (range).*
3

Characters	Female		Male
	Holotype	Paratypes	Paratype
n	–	16	1
L	789	919 ± 81.4 (758-1049)	789
a	23.2	28.3 ± 2.2 (24.4-32.8)	23.2
b	6.3	6.7 ± 0.5 (6.2-7.8)	4.6
b'	5.2	5.7 ± 0.4 (5.1-6.6)	4.5
c	37.2	41.5 ± 7.1 (32.3-55.9)	31.6
c'	1.4	1.2 ± 0.2 (0.9-1.6)	1.2
V or T	59.1	59.9 ± 2.6 (52-63)	45.2
Stylet	29.0	28.8 ± 1.6 (27-32)	26.0
Stylet conus	15.0	14.1 ± 0.8 (13-15)	12.0
DGO	8.0	8.2 ± 1.4 (6.0-11.0)	9.0
O	27.6	28.5 ± 5.1 (20.0-39.3)	34.6
Anterior end to centre of median bulb	85	90 ± 6.3 (74-99)	96
Anterior end to excretory pore	127	128 ± 13.3 (97-147)	127
Pharynx length	159	143 ± 13.2 (118-166)	170
Pharyngeal overlap	30.0	26.4 ± 4.5 (19-33)	4.0
Max. body diam.	25.0	32.7 ± 4.0 (25-40)	34.0
Anal/cloacal body diam.	16.0	18.6 ± 1.8 (16-22)	21.0
Tail	22.0	22.5 ± 3.1 (17-28)	25.0
Tail annuli	14.0	13.2 ± 1.5 (10-16)	–
Phasmid to terminus	36.0	38.8 ± 3.2 (32-43)	24
Spicules	–	–	30.0
Gubernaculum	–	–	18.0

4
5

Figure legends

Fig. 1. Rotylenchus iranicus *n. sp. A, B: Entire male and female. C: Pharyngeal region ; D, E: Gubernaculum; F: Vulval region; G: Male tail region; H-K: Female tail region.*

Fig. 2. *Photomicrographs of* Rotylenchus iranicus *n. sp. A, B: Entire female and male; C: Female pharyngeal region; D: Female anterior body region; E, F: Detail of pharyngeal glands; G: Vulval region; H: Detail of lateral field at mid-body; I-M: Female tails; N: Male tail with bursa and copulatory apparatus. Abbreviations: a = anus; ep = excretory pore; ept =epiptygma; n =nucleus of pharyngeal glands; ph = phasmid. (Scale bars: A, B = 100 µm; C-N = 20 µm.)*

Fig. 3. Rotylenchus conicaudatus *n. sp. A, B: Entire female and male. C: Pharyngeal region; D-I: Female tail regions. J: Vulval region; K-N: Pharyngeal glands; O: Male tail region.*

Fig. 4. *Photomicrographs of* Rotylenchus conicaudatus *n. sp. A: Entire female and male; B: Female pharyngeal region; C: Female anterior body region; D-F: Female tails; G: Male tail with bursa and copulatory apparatus. Abbreviations: a = anus; ep = excretory pore; n =nucleus of pharyngeal glands; ph = phasmid. (Scale bars: A = 100 µm; B = 50 µm; C-G = 20 µm.)*

Fig. 5. *The 50% majority rule consensus trees from Bayesian analysis generated from the D2-D3 of 28S rRNA gene dataset with the TVM + I + G model. Posterior probabilities more than 65% are given for appropriate clades (in bold letters); bootstrap values greater than 50% are given on appropriate clades in ML analysis. Newly obtained sequences are underlined.*

Fig. 6. *The 50% majority rule consensus trees from Bayesian analysis generated from the ITS-rRNA gene dataset with TVM + G model. Posterior probabilities more than 65% are given for appropriate clades (in bold letters); bootstrap values greater than 50% are given on appropriate clades in ML analysis. Newly*

obtained sequences are underlined. cl: indicates clone number in the original sequence.

Fig. 1.

Fig. 2.

Fig.3.

Fig. 4.

Fig. 5.

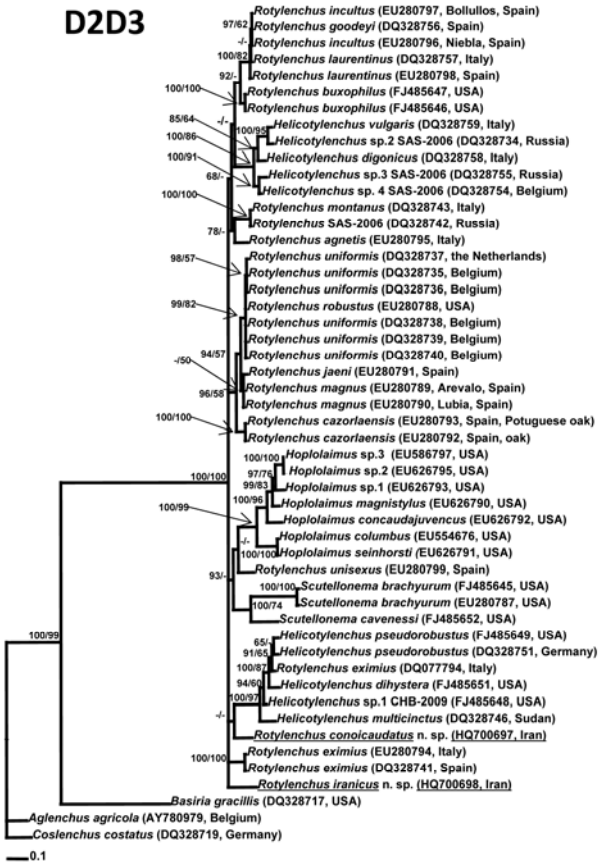
D2D3
Rotylenchus incultus (EU280797, Bollullos, Spain)
Rotylenchus goodeyi (DQ328756, Spain)
Rotylenchus incultus (EU280796, Niebla, Spain)
Rotylenchus laurentinus (DQ328757, Italy)
Rotylenchus laurentinus (EU280798, Spain)
Rotylenchus buxophilus (FJ485647, USA)
Rotylenchus buxophilus (FJ485646, USA)
Helicotylenchus vulgaris (DQ328759, Italy)
Helicotylenchus sp.2 SAS-2006 (DQ328734, Russia)
Helicotylenchus digonicus (DQ328758, Italy)
Helicotylenchus sp.3 SAS-2006 (DQ328755, Russia)
Helicotylenchus sp. 4 SAS-2006 (DQ328754, Belgium)
Rotylenchus montanus (DQ328743, Italy)
Rotylenchus SAS-2006 (DQ328742, Russia)
Rotylenchus agnetis (EU280795, Italy)
Rotylenchus uniformis (DQ328737, the Netherlands)
Rotylenchus uniformis (DQ328735, Belgium)
Rotylenchus uniformis (DQ328736, Belgium)
Rotylenchus robustus (EU280788, USA)
Rotylenchus uniformis (DQ328738, Belgium)
Rotylenchus uniformis (DQ328739, Belgium)
Rotylenchus uniformis (DQ328740, Belgium)
Rotylenchus jaeni (EU280791, Spain)
Rotylenchus magnus (EU280789, Arevalo, Spain)
Rotylenchus magnus (EU280790, Lubia, Spain)
Rotylenchus cazorlaensis (EU280793, Spain, Potuguese oak)
Rotylenchus cazorlaensis (EU280792, Spain, oak)
Hoplolaimus sp.3 (EU586797, USA)
Hoplolaimus sp.2 (EU626795, USA)
Hoplolaimus sp.1 (EU626793, USA)
Hoplolaimus magnistylus (EU626790, USA)
Hoplolaimus concaudajuvencus (EU626792, USA)
Hoplolaimus columbus (EU554676, USA)
Hoplolaimus seinhorsti (EU626791, USA)
Rotylenchus unisexus (EU280799, Spain)
Scutellonema brachyurum (FJ485645, USA)
Scutellonema brachyurum (EU280787, USA)
Scutellonema cavenessi (FJ485652, USA)
Helicotylenchus pseudorobustus (FJ485649, USA)
Helicotylenchus pseudorobustus (DQ328751, Germany)
Rotylenchus eximius (DQ077794, Italy)
Helicotylenchus dihystera (FJ485651, USA)
Helicotylenchus sp.1 CHB-2009 (FJ485648, USA)
Helicotylenchus multicinctus (DQ328746, Sudan)
Rotylenchus conoicaudatus n. sp. (HQ700697, Iran)
Rotylenchus eximius (EU280794, Italy)
Rotylenchus eximius (DQ328741, Spain)
Rotylenchus iranicus n. sp. (HQ700698, Iran)
Basiria gracillis (DQ328717, USA)
Aglenchus agricola (AY780979, Belgium)
Coslenchus costatus (DQ328719, Germany)
0.1

1 Fig.6.

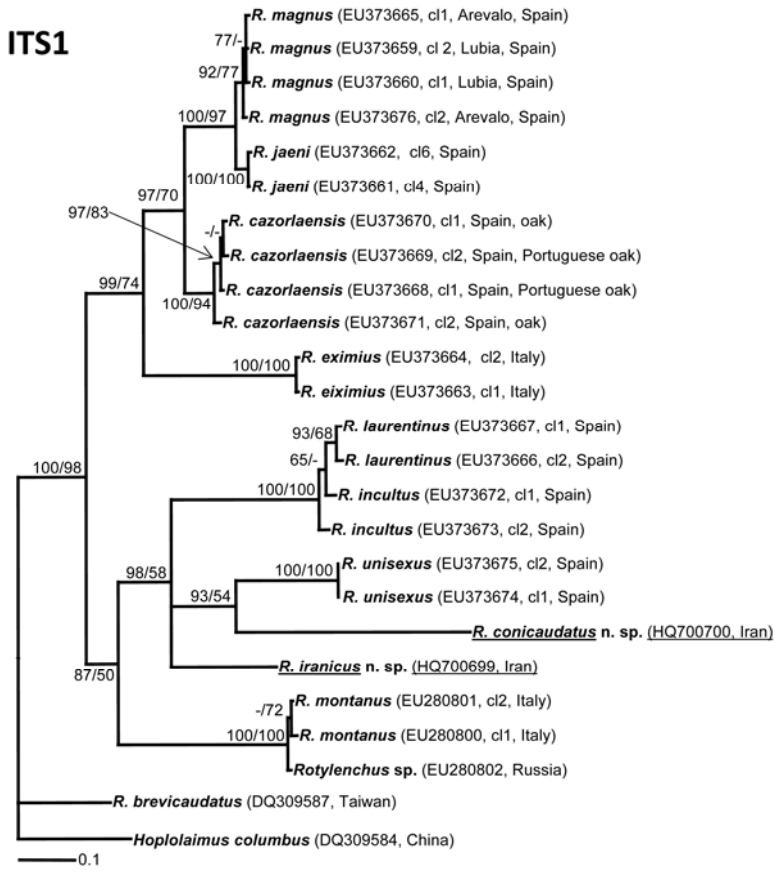
ITS1
R. magnus (EU373665, cl1, Arevalo, Spain)
77/-
R. magnus (EU373659, cl 2, Lubia, Spain)
92/77
R. magnus (EU373660, cl1, Lubia, Spain)
100/97
R. magnus (EU373676, cl2, Arevalo, Spain)
R. jaeni (EU373662, cl6, Spain)
100/100
R. jaeni (EU373661, cl4, Spain)
97/70
97/83
-/-
R. cazorlaensis (EU373670, cl1, Spain, oak)
R. cazorlaensis (EU373669, cl2, Spain, Portuguese oak)
99/74
R. cazorlaensis (EU373668, cl1, Spain, Portuguese oak)
100/94
R. cazorlaensis (EU373671, cl2, Spain, oak)
100/100
R. eximius (EU373664, cl2, Italy)
R. eiximius (EU373663, cl1, Italy)
93/68
R. laurentinus (EU373667, cl1, Spain)
65/-
R. laurentinus (EU373666, cl2, Spain)
100/98
100/100
R. incultus (EU373672, cl1, Spain)
R. incultus (EU373673, cl2, Spain)
98/58
100/100
R. unisexus (EU373675, cl2, Spain)
93/54
R. unisexus (EU373674, cl1, Spain)
R. conicaudatus n. sp. (HQ700700, Iran)
R. iranicus n. sp. (HQ700699, Iran)
87/50
-/72
R. montanus (EU280801, cl2, Italy)
100/100
R. montanus (EU280800, cl1, Italy)
Rotylenchus sp. (EU280802, Russia)
R. brevicaudatus (DQ309587, Taiwan)
Hoplolaimus columbus (DQ309584, China)
0.1

2